EBMBDT: Effective Block Matching Based Denoising Technique using Dual Tree Complex Wavelet Transform

M. Selvi
Aloy Labs, I-901, Springfields Apts, Sarjapur Road, Bellandur Gate, Bangalore – 560102, India

Abstract. In processing and investigation of digital image denoising of images is hence very important. In this paper, we propose a Hybrid de-noising technique by using Dual Tree Complex Wavelet Transform (DTCWT) and Block Matching Algorithm (BMA). DTCWT and BMA is a method to identify the noisy pixel information and remove the noise in the image. The noisy image is given as input at first. Then, bring together the comparable image blocks into the load. Afterwards Complex Wavelet Transform (CWT) is applied to each block in the group. The analytic filters are made use of by CWT, i.e. their real and imaginary parts from the Hilbert Transform (HT) pair, defending magnitude-phase representation, shift invariance, and no aliasing. After that, adaptive thresholding is applied to enhance the image in which the denoising result is visually far superior. The proposed method has been compared with our previous de-noising technique with Gaussian and salt-pepper noise. From the results, we can conclude that the proposed de-noising technique have shown better values in the performance analysis.

Key words: image denoising, Complex Wavelet Transform (CWT), dual tree CWT, block matching, soft thresholding.

1. Introduction

For image processing researchers for a lengthy period, Image denoising is a dynamic area of interest. Image denoising plans at lessening the noise in homogeneous areas whereas saving the image contours. For post processing techniques like segmentation, classification, object recognition, pattern analysis, registration, etc, Image denoising is significant [19]. The noise of image is not generally effortlessly eradicated in image processing. According to image characteristic, Noise statistical property and frequency spectrum allocation rule really computed, there are many researchers improved several techniques of eliminating noises that roughly are separated into space and transformation fields. The space field is information operation brought on the initial image, and processes the image gray value, like neighborhood average technique, Total Variation (TV) filter, ROF filter, wiener filter and so on [16]. Several dissimilar cases of alterations are there. One of the most common cases is alteration owing to preservative white Gaussian noise which can be caused by poor image achievement or by transmitting the image data in noisy communication channels. Other kinds of noises consist of impulse and speckle noises. A denoising algorithm has to acclimatize to image discontinuities in order to accomplish a good presentation in this reverence. For image denoising, Wavelet

transforms have been applied successfully supplying a means to utilize the relationships among coefficients at numerous scales [11].

To take away the noise while holding as much as feasible the significant signal features is the goal of denoising. Image denoising still stays a challenge for researchers since noise elimination launches artifacts and causes blurring of the images. To carry out denoising of images, numerous techniques are being improved [14]. Two fundamental strategies are there to image denoising, spatial filtering techniques and change domain filtering techniques. Spatial filters use a low pass filtering on groups of pixels with the statement that the noise absorbs the higher area of frequency spectrum. Spatial Low-pass filters will not just level away noise however moreover blur edges in signals and images while the high-pass filters can compose edges still sharper and develop the spatial resolution however will furthermore enlarge the noisy background [1]. Linear filters, which contain convolving the image with a steady matrix to attain a linear mixture of neighborhood values, have been extensively applied for noise removal in the existence of additive noise [15].

From the computational point of outlook, the discrete transform is incredibly competent. Wavelets provide a better presentation in image denoising owing to properties such as sparsity and multi resolution structure. It engages three steps: a linear forward wavelet transform, nonlinear thresholding step and a linear inverse wavelet transform. Wavelet thresholding (first suggested by Donoho [4]) is a signal evaluation method that utilizes the capabilities of wavelet transform for signal denoising. By killing coefficients, it takes away noise that are unimportant relative to some threshold, and turns out to be easy and efficient, depends heavily on the selection of a thresholding parameter and the selection of this threshold concludes, to a huge degree the effectiveness of denoising. Directional wavelet transforms [3]; steerable pyramids [2], complex wavelets [5], curvelets [6] and contourlets [9] are some examples where all of them are unneeded. Although the Discrete Wavelet Transform (DWT) is a dominant image and signal-processing device, it has three drawbacks that destabilize its usage in several applications.

Initially, it is shift responsive since input-signal shifts produce unpredictable alterations in DWT coefficients. Next, the DWT endures from poor directionality since DWT coefficients expose only three spatial points of references. Third, DWT study of real signals needs the phase data that precisely explains non-stationary signal performance. The Dual-Tree Wavelet Transform (DTWT) was produced by Kingsbury [5], [8] to overcome these problems, which is a redundant, complex wavelet transform with outstanding directionality, diminished shift sensitivity and clear phase information. The DTWT gives up superb results in applications where idleness is tolerable because of these benefits [8], [10]. The DTWT is outmoded since it contains a pair of filter banks that concurrently work on the input signal and offer two wavelet disintegrations. The wavelets related with the filter banks are a Hilbert pair. This asset is significant because it offers the benefits of reduced shift sensitivity, enhanced directionality and clear phase

information. Conversely, the aim of Kingsbury's DTWT filters is difficult since it needs an iterative optimization over the space of perfect-reconstruction filter banks.

The decisively modeled Discrete Wavelet Transform (DWT) has been effectively used to an extensive range of image denoising tasks. Though, because of the subsequent problems, its presentation is restricted [7]. The double-tree CWT is an important improvement of the traditional actual wavelet transform that is almost shifting invariant and, in elevated dimensions, directionally selective. As the actual and imaginary parts of the dual-tree CWT are, in truth, conservative real wavelet changes the CWT advantages from the vast theoretical, practical, and computational resources that have been progressed for the standard DWT [7], [12], [13].

Several works are available in the literature for the image de-noising using medical and other images. However, in the neighborhood of discontinuities, linear filtering such as the Gaussian filter removes noise but blurs edges significantly. This undesirable effect can be reduced by considering local geometries and statistics during the filtering process. In this work, we proposed an efficient denoising technique using DTCWT based on block matching algorithm. Here, block matching process is used in order to overcome the smoothing filter type and it will not affect the lower dimensions. Then DTCWT and adaptive thresholding are used for the image denoising and image enhancement phase. Finally, PSNR and SDME are used for the evaluation matrices. The rest of the paper is organized as follows: a brief review of some of the literature works in denoising technique is presented in Section 2. The proposed image denoising technique is detailed in Section 3. The experimental results and performance evaluation discussion is provided in Section 4. Finally, the conclusions are summed up in Section 5.

2. Related Works

For image denoising, a handful of researches have been offered in the literature. Lately, applying Dual Tree Complex Wavelet Transform (DTCWT) for image denoising has obtained a huge deal of awareness among researchers. A short assessment of some new researches is offered in Tab. 1.

3. Image Denoising Using Complex Wavelet Transform and Block Estimation

In the area of image processing, Image Denoising has continued a basic problem. Due to numerous inevitable reasons, it is not unusual that images are polluted by noise. When applying Complex Wavelet Transform (CWT), emphasized that matter such as selection of primary resolution (the scale level at which to begin thresholding) and selection of analyzing wavelet moreover have a great pressure on the victory of the shrinkage process. In such a wavelet transform, a great magnitude of a coefficient implies the existence of a singularity while the phase indicates its location inside the support of the wavelet.

Tab. 1. Set of selected researches and their works.

Authors	**Year**	**Algorithm**	**Purpose**	**Difference of our work**
Tamanna Howlader and Yogendra P. Chaubey [17]	2010	Complex wavelet Transform	Denoising of cDNA microarray images	Works well only on micro array images.
Benjamin Huhle et al. [18]	2010	Non Local Means	Denoising and resolution enhancement	Computationally expensive.
Rodrigo Moreno et al. [21]	2011	Tensor voting frame work	Denoising and surface reconstruction	It will remove the noise only on edge regions
Chen et al. [22]	2012	Dual tree complex wavelets	Image denoising	
Xiang-Yang Wang et al. [26]	2014	Extended discrete shear let transform, Hidden Markov Tree	Edge preserving denoising scheme	Works well only on localvar noise
Lakshmi Srinivasan et al. [25]	2014	Complex Gaussian scale mixture (CGSM) model, complex wavelet transform	Two channel micro array images denoising	Works well only on micro array images.
Norbert Remenyi et al. [24]	2014	Complex wavelet transform, bayes estimation	Image denoising	It will works only in diagonal shrinkage method.
Amel Baha Houda et al. [23]	2015	Dual tree complex wavelets	Medical image denoising	They are concentrated only on Blocky images
Ayushi Jaiswal et al. [27]	2014	Discrete Wavelet Transform	Image denoising	The proposed method works only in salt and pepper noise and Gaussian noise.

The complex wavelet transform (CWT) uses analytic or quadrature wavelets promising magnitude- phase illustration, shift invariance and no aliasing. A competent way of suggested denoising method is explained by Fig. 1.

Let us regard the noisy image $z : X \to R$ of the form, i.e.,

$$z(x) = y(x) + \eta(x) \tag{1}$$

Let us introduce the inspection model and memo applied right through the paper. We consider noisy observations $z : X \to R$ of the form $z(x) = y(x) + \eta(x)$, where $x \in X$ is 2D spatial coordinating that belongs to the image domain $X \subset Z^2$, y is the true image, and $\eta(x) \approx \aleph(0, \sigma^2)$, is white Gaussian noise of variance σ^2. By Z_x we indicate a block of fixed size $M \times N$ removed from z, which has $z(x)$ as its upper-left element; instead, we say that Z_x is situated at x. With $\hat{y}$ we assign the last estimate of the true image.

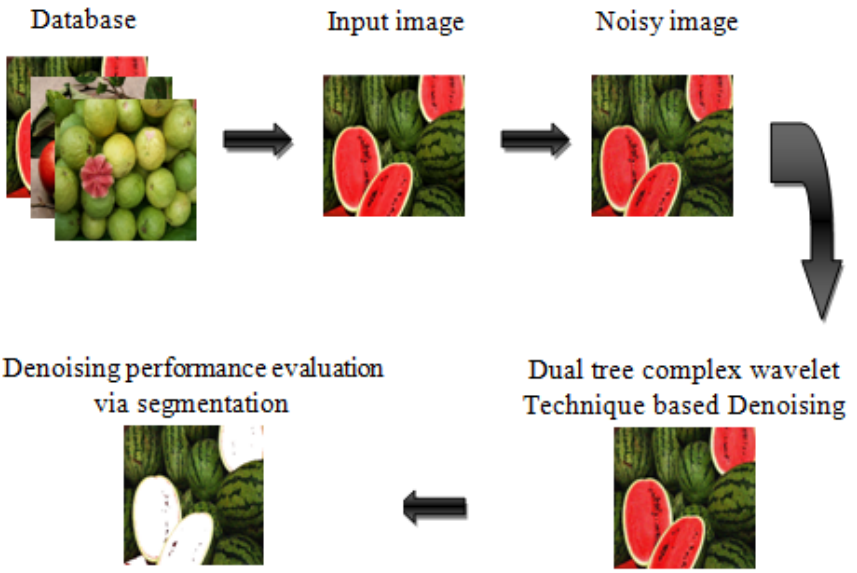

Fig. 1. Block diagram of the Proposed Method.

Let us utter the applied statements. We take for granted that some of the blocks (of fixed size $M \times N$) of the true image show mutual relationship. We moreover assume that the chosen unitary transform is able to signify sparsely these blocks. Let z be an image of dimension $M \times N$. Partition the image z into number of $M \times N$ non overlapping blocks. This can be signified as

$$z = \{zb_1, zb_2, ..., zb_{Nb}\} \tag{2}$$

where Nb signifies the total number of blocks in the image. Next, the related block from the image is recognized by applying the block matching process.

3.1. Block Matching

The property of self-similarity of objects is applied by block matching procedure in image and video compression. A few of the blocks acquired by dividing the image into numerous blocks are alike. Hence, the idea of block matching is applied to stop executing repetitive denoising on the similar block. Using block matching, related blocks in a specified input image are recognized i.e., the matched blocks for every indication block in an image. To compute the resemblance between the images, the Euclidean distance measure is applied.

Our suggested technique [20], computes the similarity of the a^{th} block for the block matching procedure by comparing the distance measure of the a^{th} block and its n neighboring blocks. Equation 3 is applied to compute the distance measure,

$$S_d = \sqrt{\sum (zb_a - zb_b)^2} \tag{3}$$

here Ib_a and Ib_b, where $b = \{1, 2, ..., n\}$, signify the current block and blocks next to the current block, correspondingly. This is illustrated in the Fig. 2.

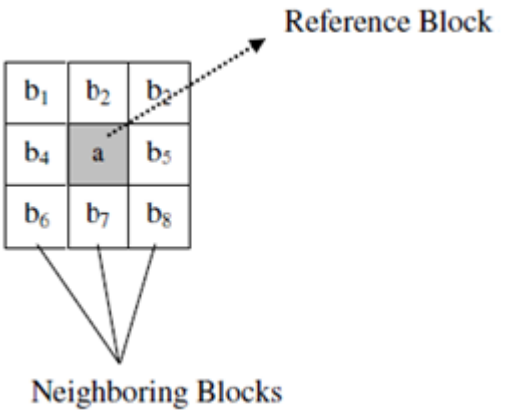

Fig. 2. Reference blocks and adjacent blocks.

The flag value is placed according to the threshold D_tsh, following the distance measure is computed. The computed distance S_d is compared with the threshold D_tsh as follows,

$$I_F^b = \begin{cases} I_F^b = 1; & if S_d < D_{tsh} \\ I_F^b = 0; & otherwise \end{cases} \tag{4}$$

Here b and F signify the image block and the flag value of every block of the image, correspondingly. Both a^{th} and b^{th} blocks are said to be alike if the b^{th} block yields a flag value of 1, when it is compared with the a^{th} block. Or else they are said to be different. This is shown in Fig. 3.

Hence we accumulate the indices by recognizing the blocks related to the a^{th} block. In fractal image compression, a^{th} block is the array block and the analogous similar blocks are domain blocks. As a substitute of all the similar domain blocks, we apply only the sort block once the indices of range block and its related domain blocks are

1	1	0
1	a	0
1	0	0

Fig. 3. Flags assigned to each domain blocks.

gathered. The time and memory difficulty is reduced by this. After joining the similar blocks into a heap, CWT is used to the domain blocks in each of the group.

3.2. Complex Wavelet Transform (CWT)

The image with the initial guessing pixel values is given to 2D dual tree M band wavelet transform, which offers local, multi-scale and directional analysis. The M- band multi-resolution analysis of $L^2(R)$ with $M \geq 2$ is defined by one scaling function (or father wavelet) $\psi \in L^2(R)$ and $M-1$ mother wavelets $\psi_m \in L^2(R), m \in \{1, ..., M-1\}$. These functions are the solution of the following scaling equation:

$$\frac{1}{M^{\frac{1}{2}}} \psi\, m\left(\frac{s}{\sqrt{M^2}}\right) = \sum_{k=-\infty}^{\infty} f_m[g]\psi_0(s-g) \tag{5}$$

where, $(f_m\,[g])_{g\in z}$ are the square summable sequences. In the following, we will assume that these functions (and thus the associated sequences $(f_m\,[g])_{g\in z}$ are real valued. The Fourier transform of $(f_m\,[g])_{g\in z}$ is a 2π periodic function, represented by H_m for the set of functions $\left(\bigcup_{m=1}^{M-1}\{M^{-j/2}\,\psi_m(M^{-j}s-g), (j,g)\in Z^2\}\right)$ to correspond to an orthonormal basis of $L^2(R)$, and the following paraunitary conditions should hold:

$$\sum_{p=0}^{M-1} H_m \frac{(wM+pM+2\pi)}{M} H^*_{m'} \frac{(wM+pM+2\pi)}{M} = M\lambda_{m-m'} \tag{6}$$

where, $\lambda_m = 1$ if $m = 0$ and 0 otherwise. Our aim is to build a "dual" M-band multi resolution analysis defined by scaling function ψ_0^H and mother wavelets $\psi_m^H, (m \in \{1, 2, ..., M-1\}$ More accurately, the mother wavelets will be obtained by means of a Hilbert transform from the "original" wavelets $\psi_m, m \in \{1, 2, ..., M-1\}$. In the Fourier domain, the desired property reads

$$\forall m \in \{1, ..., M-1\},\ |\hat{\psi}_m^H(w)| = -i\ sign(w)\,\hat{\psi}(w) \tag{7}$$

where, $(f_m\,[g])_{g\in Z}$ sign is the signum function, and $\hat{d}$ is the fourier transform of the function d. Moreover, the functions $\hat{\psi}_m^H$ are defined by scaling equations similar to (5)

involving real - valued sequences $(f_m[g])_{g\in Z}$. In order to create dual M-band orthonormal wavelet basis of $L^2(R)$, the Fourier transform G_m of the sequences $(f_m[g])_{g\in Z}$ should satisfy the paraunitary conditions. The Hilbert condition 8 yields

$$\forall m \in \{1, ..., M-1\} \qquad |\hat{\psi}_m^H(w)| = |\hat{\psi}_m(w)| \tag{8}$$

The scaling equation leads to

$$\forall m \in \{1, ..., M-1\} \qquad G_m(w) = e^{-i\theta m(w)} H_m(w) \tag{9}$$

where θ_m is 2π periodic. The frequency phase functions should also be odd (for real filters) and thus only need to be determined over $[0, \pi]$. In the 2-band case (under weak assumptions), θ_m is a linear function on $[-\pi, \pi]$. In the M band case, the constraint is slightly restricted on a smaller interval by imposing $\forall w \in [0, 2\pi/M],\ \theta_0(w) = \zeta w$, where $\zeta \in R$.

It can be deduced that, paraunitary M band filter bank conditions are obtained by selecting the phase functions defined by eqn 10,

$$\forall p \in \{0, ..., \left(\frac{M}{2}\right) - 1\}, \forall w \in \left[\frac{pM + 2\pi}{M}, (p+1)\frac{2\pi}{M}\right], \theta_0 = \left(d + \frac{1}{2}\right)(M-1)w - p\pi, \tag{10}$$

$$\forall m \in \{1, ..., M-1\}, \theta_m(w) \in \begin{cases} \frac{\pi}{2} - (d + \frac{1}{2})w & \text{if } w \in (0, 2\pi], \\ 0 & \text{if } w = 0, \end{cases} \tag{11}$$

where $d \in Z$ denotes the upper integer part of real u. The scaling function related to the dual wavelet composition is such that

$$\forall k \in N, \forall w \in [2k\pi, 2(k+1)\pi, \hat{\psi}_0^H(w) = (-1)^k e^{-1\left(d+\frac{1}{2}\right)w} \psi_0(w) \tag{12}$$

It should also be noted that except for the 2 band case, θ_0 exhibits discontinuities on $0, \pi$ due to the $p\pi$ term.

The 2D separable M-band wavelet bases are derived from the 1D dual tree decomposition. Thus, we obtained two bases of $L^2(R^2)$. The first one corresponds to the conventional 2D separable wavelet basis, but the second one results from the tensor product of the dual wavelet basis function. A discrete implementation of these wavelet decomposition starts from the level $j = 1$ to the coarsest resolution level $j \in N^*$. The decomposition on the former 2D wavelet basis function yields coefficients $\delta_{j,m,m'}[k, l]$, whereas the decomposition on the dual basis generates coefficients $\delta_{j,m,m'}[k, l]$.

3.3. Soft Thresholding

After using CWT to the domain blocks of the group, soft thresholding method is employed to denoise the blocks. In this suggested method, Normal Shrink is applied as soft

thresholding to denoise the noise blocks. The suggested technique executes soft thresholding with the data driven subband dependent threshold T_N which can be specified as,

$$T_N = \frac{\beta\hat{\sigma}^2}{\hat{\sigma}_y} \tag{13}$$

where,

β is the scale parameter,
$\hat{\sigma}^2$ is the noise variance,
$\hat{\sigma}_y$ is the standard deviation of the subband under consideration computed, by using the standard equation.

The scale parameter β is computed once for each scale using the following equation

$$\beta = \sqrt{\log\left(\frac{L_k}{J}\right)} \tag{14}$$

where,

L_k is the length of the sub band at k^{th} scale.

The noise variance $\hat{\sigma}^2$ can be calculated is from the subband HH1, using the formula

$$\hat{\sigma}^2 = \left[\frac{\text{median}\left(|Y_i j|\right)^{-2}}{0,6745}\right], Y_i j \in \text{sub band HH1} \tag{15}$$

After applying the soft thresholding to the noisy blocks, inverse CWT must be applied to rearrange the blocks.

3.4. Inverse CWT

Using the opposite complex wavelet transform, the resulting fused image is next generated by changing the united coefficient map. The wavelet coefficient images demonstrate the orientated nature of the complex wavelet subbands. Consequently the denoised image attained after the procedure of using converse complex wavelet transform.

4. Results and Discussion

In this section, we illustrate the effectiveness of the proposed scheme in image denoising by means of the results obtained from the experimentation. The proposed method was implemented in MATLAB (Matlab 7.13) and the proposed hybrid coding scheme was evaluated using both grayscale and color images. The test images used in the experiments

include: Lena, Barbara, Baboon, Peppers, Balloon, and Apple etc. The quality of the denoised images was determined by measuring the PSNR values and SDME values. The sample output obtained from the proposed method is presented in Tab 2.

In the figures 4, 5 and 6, the image is segmented based on red color. The efficiency of segmentation of denoised image is demonstrated beneath. The precision of the segmentation is more as compared to the segmentation ok noisy image. From the figures 4, 5 and 6, we can illustrate the significance of image denoising for image segmentation.

At this point we are applying three methods to compare the segmentation presentation of the image. These are

1. Rand Index,
2. Global Consistency Error,
3. Variation Index.

If the Rand Index is elevated, the segmentation presentation is excellent. The Global Consistency Error must be little to get improved segmentation result. The value of Variation Index must be fewer to generate improved segmentation. Tab. 3 and Fig. 7 demonstrates the efficiency of segmentation of noised and denoised image.

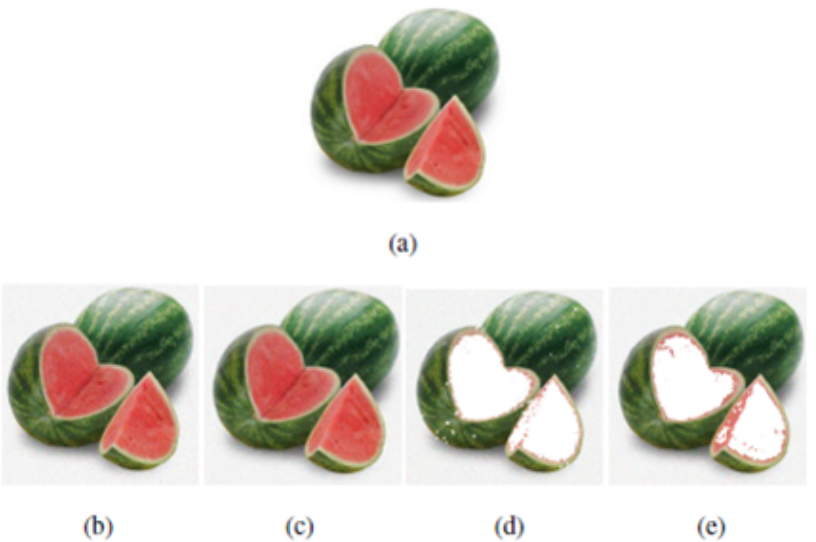

Fig. 4. Importance of Denoising (a) original image (b) noisy image (c) denoised image (d) noisy image segmentation (e) denoised image segmentation.

Tab. 2. Denoised image output.

Original image	**Noisy image**	**Denoised image**
		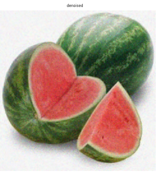
		
		
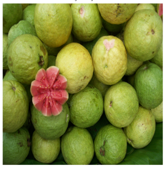		
		
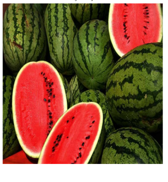		

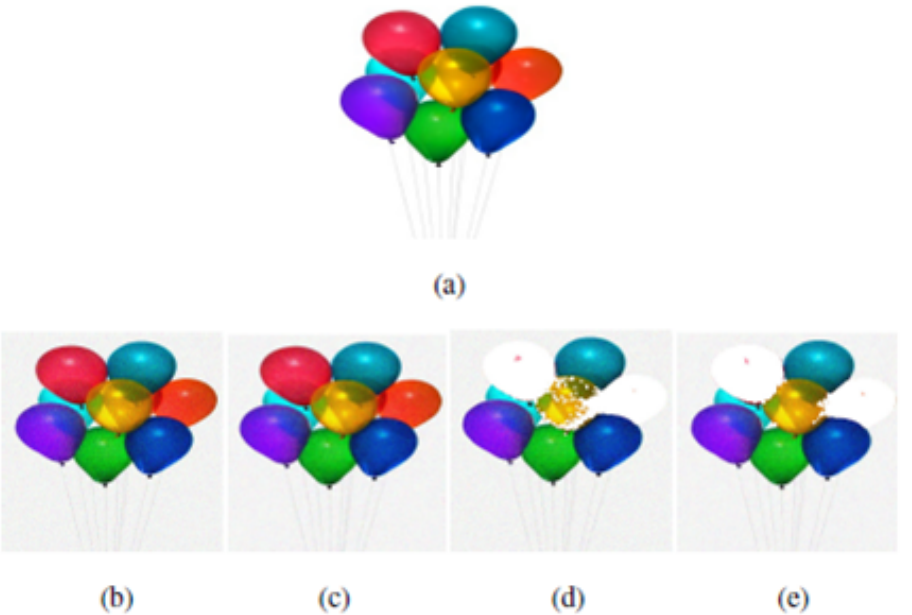

Fig. 5. Importance of Denoising (a) original image (b) noisy image (c) denoised image (d) noisy image segmentation (e) denoised image segmentation.

Tab. 3. Segmentation Comparison

Methods	Denoised Image	Noisy image
Rand Index (RI)	0.8121	0.6898
Global Consistency Error (GCE)	0.000022888	0.0177
Variation of Information (VI)	3.2990	4.3616

4.1. Comparative Analysis

The formulae used to compute the evaluation metrics PSNR and SDME values are given as follows:

Peak Signal to Noise Ratio (PSNR) The formula for PSNR value computation is,

$$\text{PSNR} = 10 \log_{10} \frac{E_{max}^2 \times I_w \times I_h}{\sum (I_{xy} - I_{xy}^*)} \tag{16}$$

where, I_w and $I_h \rightarrow$ Width and height of the de-noised image, $I_{xy} \rightarrow$ Original image

Fig. 6. Importance of Denoising (a) original image (b) noisy image (c) denoised image (d) noisy image segmentation (e) denoised image segmentation.

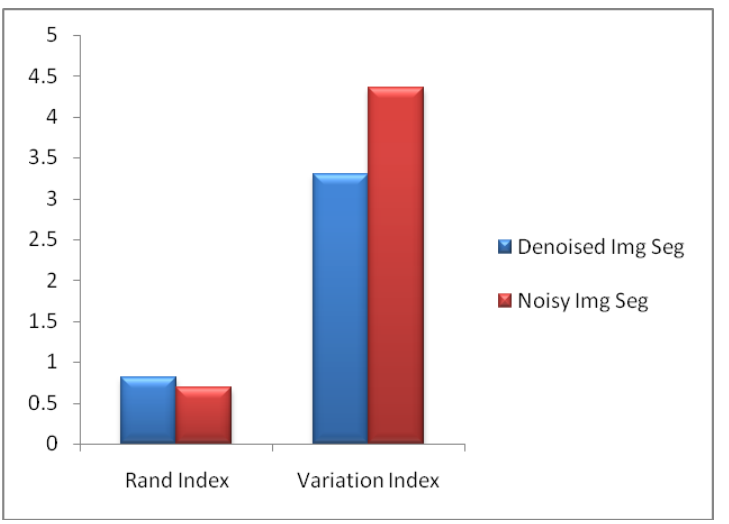

Fig. 7. Segmentation Comparison.

pixel value at coordinate (x, y), $I^*_{xy} \rightarrow$ De-noised image pixel value at coordinate (x, y), $E^2_{max} \rightarrow$ Largest energy of the image pixels.

Second-Derivative Measure of Enhancement (SDME) The formula for SDME value computation [15] is,

$$\text{SDME} = -\frac{1}{k_1 k_2} 20 \ln \left| \frac{I_{max;k,l} - 2I_{center;k,l} + I_{min;k,l}}{I_{max;k,l} + 2I_{center;k,l} + I_{min;k,l}} \right| \tag{17}$$

where the de-noised image is divided into $(k_1 \times k_2)$ blocks with odd size, $I_{max;k,l}$ and $I_{min;k,l}$ corresponding to the maximum and minimum values of pixels in each block whereas $I_{center;k,l}$ is the value of the intensity of the pixel in the center of each block.

Tab. 4 shows the comparison of PSNR and SDME values at various noise levels. The denoised output of the images for colored and gray scale images by ordinary DWT technique and suggested methods is illustrated in Fig. 8 and Fig. 9.

Tab. 4. PSNR and SDME comparison




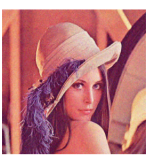

Noise level	PSNR	SDME	PSNR	SDME	PSNR	SDME	PSNR	SDME
0.2	29.77923	92.02004	19.7439	93.1990	25.48929	81.79186	27.93929	87.21707
0.4	28.64254	86.91706	27.5100	90.44937	25.021	81.2642	26.8411	87.6524
0.6	28.22196	85.30869	27.6063	88.6106	24.65612	81.6432	25.9541	87.625
0.8	26.124	81.2356	26.489	86.1236	23.5516	81.2692	24.8782	87.5124
1.0	25.487	79.3654	25.985	82.3642	22.98454	81.3645	23.6423	87.35845

Fig. 8 and Fig. 9 shown that the suggested system presents improved presentation when compared to the ordinary DWT technique. The visuality of the improved image of suggested technique is high. The PSNR comparison is explained as follows.

Tab. 5 presents the values of the PSNR for both DWT and the suggested CWT technique for Lena and Pepper images. Fig. 10 illustrates the efficiency of the suggested technique as compared with normal DWT technique.

Tab. 5. The PSNR values for both DWT and CWT

Denoising methods	Lena	Peppers
DWT	28.12	28.43
CWT	33.45	32.17

Fig. 8. Comparison of Proposed method with existing DWT (a) Input noisy image (b) Denoising using ordinary DWT (c) Proposed method output.

5. Conclusion

Using Dual tree Complex Wavelet Transform, our document explains the idea of de-noising the images. The dual-tree CWT is an important improvement of the traditional real wavelet transform that is almost shifting invariant and, in elevated dimensions, directionally choosy. As the actual and imaginary fractions of the dual-tree CWT are, in reality, conventional real wavelet changes the CWT advantages from the vast theoretical, practical, and computational resources that have been improved for the standard DWT. In this research, we applied block matching method to recognize the related blocks to diminish the time consumption. The image denoising algorithm employs soft thresholding to offer smoothness and enhanced edge preservation. The suggested algorithm is checked with numerous kinds of images and the result demonstrates that the produced output images are enhanced in quality with less noise. The comparison of the de-noising results on natural images indicated that the proposed technique outperformed the other one in terms of the objective PSNR and SDME values and the visual quality assessment.

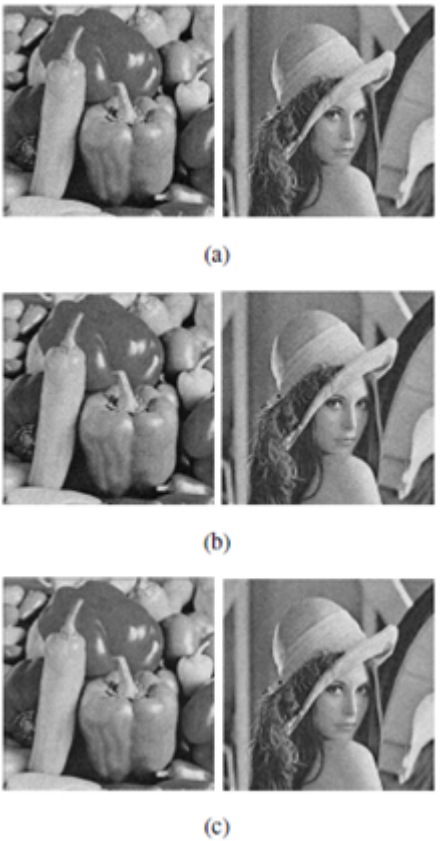

Fig. 9. Comparison of Proposed method with existing DWT (a) Input noisy image (b) Denoising using ordinary DWT (c) Proposed method output.

References

1985

[1] McVeigh E. R., Henkelman R. M., Bronskill M. J.: Noise and filtration in magnetic resonance imaging. Med. Phys., 12(5):586-591.

1992

[2] Simoncelli E. P., Freeman W. T., Adelson E. H., Heeger D. J.: Shiftable multi-scale transforms. IEEE Transaction of Information Theory, 38(2):587-607.

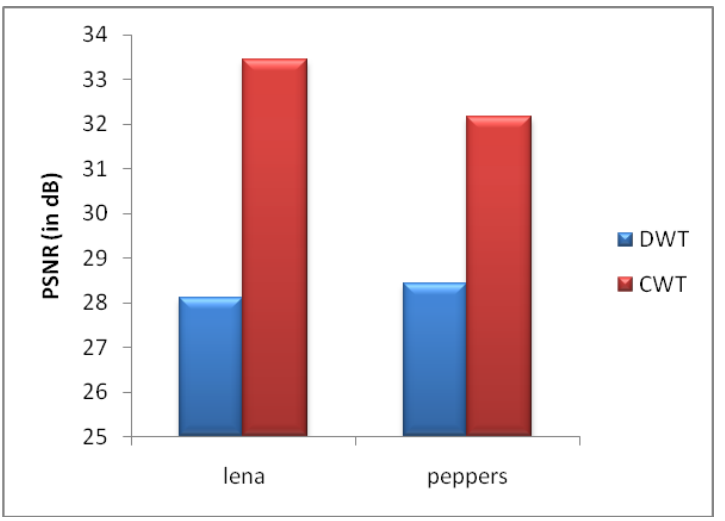

Fig. 10. PSNR Comparison.

1993

[3] Antoine P., Carrette P., Murenzi R., Piette B.: Image analysis with two-dimensional continuous wavelet transform. Signal Processing, 31:241-272.

1995

[4] David L. Donoho: De-noising by soft thresholding. IEEE Transactions on Information Theory, 41(3):613-627.

1999

[5] Candes E. J., Donoho D.: Curvelets – a surprisingly effective non adaptive representation for objects with edges. In: Curve and Surface Fitting, Saint-Malo, Vanderbuilt University Press.

[6] Kingsbury N.: Image processing with complex wavelets. Phil. Trans. R. Soc. London, UK.

[7] de Rivaz P., Kingsbury N.: Complex wavelet features for fast texture image retrieval. In: Proc. of the IEEE International Conference in Image Processing.

2000

[8] Kingsbury N.: Complex wavelets for shift invariant analysis and filtering of signals. Applied and Computational Harmonic Analysis.

2001

[9] Do M. N.: Directional multiresolution image representations. Ph.D. thesis, EPFL, Lausanne, Switzerland.

2002

[10] Romberg J. K., Choi H., Baraniuk R. G., Kingsbury N. G.: Hidden Markov tree models for complex wavelet transforms. IEEE Transactions on Signal Processing.

2005

[11] Gnanadurai D., Sadasivam V.: An efficient adaptive thresholding technique for wavelet based image denoising. International Journal of Signal Processing, 2(2):114-119.

[12] Marusic S., Deng G., Tay D.: Image Denoising Using Over-Complete Wavelet Representations. In: Proc. of the 13th European Signal Processing Conference, Antalya, Turkey.

[13] Selesnick I. W., Baraniuk R. G., Kingsbury N. G.: The Dual-Tree Complex Wavelet Transform. IEEE Signal Processing Magazine, 22(6):123-151.

2007

[14] Arivazhagan S., Deivalakshmi S., Kannan K.: Performance Analysis of Image Denoising System for different levels of Wavelet decomposition. International Journal of Imaging Science and Engineering (IJISE), 1(3):104-107.

2008

[15] Kachouie N. N.: Image Denoising Using Earth Mover's Distance and Local Histograms. International Journal of Image Processing, 4(1):66-76.

2010

[16] Aliaa A. A. Youssif, Darwish A. A., Madbouly A. M. M.: Adaptive Algorithm for Image Denoising Based on Curvelet Threshold. IJCSNS International Journal of Computer Science and Network Security, 10(1):322-328.

[17] Howlader T., Chaubey Y.P.: Noise Reduction of cDNA Microarray Images Using Complex Wavelets. IEEE Transactions On Image Processing, 19(8).

[18] Huhle B., Schairer T., Jenke P., Straßer W.: Fusion of range and color images for denoising and resolution enhancement with a non-local filter. Computer Vision and Image Understanding, 114:1336-1345.

[19] Palhano Xavier de Fontes F., Barroso G. A., Coupe P., Hellier P.: Real time ultrasound image denoising. Journal of Real-Time Image Processing, 2:1-14.

2012

[20] Chandan R., Sukadev M. A.: Hybrid Image Compression Scheme Using DCT and Fractal Image Compression. The International Arab Journal of Information, 10(6).

2011

[21] Moreno R., Garcia M. A., Puig D., Julià C.: Edge-preserving color image denoising through tensor voting. Computer Vision and Image Understanding, 115:1536-1551.

2012

[22] Chen G., Zhu W.P., Xie W.: Wavelet-based image denoising using three scales of dependency. IET Image Processing, 6(6):756-760.

2014

[23] Jaiswal A., Upadhyay J., Somkuwar A.: Image denoising and quality measurements by using filtering and wavelet based techniques. Int. J. Electron. Commun. (AEÜ), 68(8):699-705.

[24] Remenyi N., Nicolis O., Nason G., Vidakovic B.: Image Denoising With 2D Scale-Mixing Complex Wavelet Transforms. IEEE Transactions On Image Processing, 23(12):5165-5174.

[25] Srinivasan L., Rakvongthai Y., Oraintara S. : Microarray Image Denoising Using Complex Gaussian Scale Mixtures of Complex Wavelets. IEEE Journal Of Biomedical And Health Informatics, 18(4):1423-1430.

[26] Wang X.-Y., Liu Y.-C., Yang H.-Y. : Image denoising in extended Shearlet domain using hidden Markov tree models. Digital Signal Processing, 30:101-113.

2015

[27] Adamou-Mitiche A. B. H., Mitiche L., Naimi H. : Medical image denoising using dual tree complex thresholding wavelet transform and Wiener filter. Journal of King Saud University – Computer and Information Sciences, 27(1):40-45.